



OPEN

Identification of topological alterations using microstate dynamics in patients with infantile epileptic spasms syndrome

Seong-Ho Ahn^{1,6}, Han Na Jang^{2,6}, Seeun Kim³, Min-Jee Kim⁴, Mi-Sun Yum⁴✉ & Dong-Hwa Jeong^{1,5}✉

Infantile epileptic spasm syndrome (IESS) is characterized by clustered epileptic spasms and hypsarrhythmia on electroencephalography (EEG). This study aimed to investigate the temporal dynamics and dynamic synchronization of neural networks in IESS using EEG microstate analysis of interictal recordings from 49 healthy controls (HC) and 42 patients with IESS. Five microstate maps were identified, and features including the global explained variance (GEV), mean correlation, occurrence, time coverage, mean time duration, and transition probabilities were extracted. Significant differences were observed in patients with IESS compared to HCs, with increased microstate features and transition probabilities in microstates A and B, and reduced values in microstates D and E. Furthermore, in patients with structural/metabolic etiologies, microstate A demonstrated heightened microstate features and transition probabilities compared to genetic/unknown etiologies. These microstate characteristics enabled accurate classification of IESS versus HCs and differentiation between structural/metabolic and genetic/unknown etiologies. The altered microstate topologies in IESS reflect disruptions in brain network dynamics, suggesting that specific microstate features and transition probabilities could serve as potential diagnostic biomarkers. This study underscores the potential of EEG microstate analysis in understanding neural dysfunction, particularly in structural/metabolic subtypes of IESS.

Keywords Infantile epileptic spasm syndrome (IESS), West syndrome, EEG microstates, IESS etiology, Machine learning

Infantile epileptic spasm syndrome (IESS) is a severe form of epilepsy characterized by clustered epileptic spasms, developmental disabilities, and hypsarrhythmia on electroencephalography (EEG)¹. Analyzing and interpreting EEG signals is crucial for the diagnosis and monitoring of infantile spasms, as well as to understand the underlying neurophysiology. Recent neurophysiological studies using brain imaging and EEG analyses have shown that patients with epilepsy exhibit disrupted brain networks and abnormal brain connectivity².

In prior studies using resting-state functional magnetic resonance imaging (fMRI) in patients with IESS, the authors focused on identifying neurophysiological and neuroanatomical alterations, showing disrupted connectivity^{3,4}. Additional studies have shown varying treatment responses to adrenocorticotrophic hormone (ACTH) or corticosteroids in terms of brain connectivity⁵, showing how early disruptions in brain networks during critical developmental periods can influence patient outcomes⁶.

EEG is widely employed to analyze neurophysiological patterns in children due to its safety and non-invasiveness. In contrast to MRI, which requires longer test durations and specialized equipment and space, EEG can efficiently record the electrical activity of the brain, revealing rapid dynamic changes in neuronal networks, making it particularly suitable for pediatric assessments.

¹Department of Artificial Intelligence, The Catholic University of Korea, 43 Jibong-ro, Bucheon 14662, Gyeonggi-do, Republic of Korea. ²Department of Pediatrics, Soonchunhyang University Cheonan Hospital, Cheonan, Republic of Korea. ³Weldon School of Biomedical Engineering, Purdue University, West Lafayette, USA. ⁴Department of Pediatrics, Asan Medical Center Children's Hospital, Ulsan University College of Medicine, 88 Olympic-ro 43-gil, Songpa-gu, Seoul 05505, Republic of Korea. ⁵Department of Healthcare and Artificial Intelligence, The Catholic University of Korea, Bucheon, Republic of Korea. ⁶Seong-Ho Ahn and Han Na Jang contributed equally to this work. ✉email: misun.yum@gmail.com; donghwa@catholic.ac.kr

EEG microstates, obtained from multi-channel scalp recordings, reflect quasi-simultaneous activity between large-scale network nodes and the dynamic synchronization of subunits within functional networks⁷. Microstate analysis has been applied to various neuropsychiatric disorders, including schizophrenia, dementia, depression, and epilepsy⁸.

While several prior studies have analyzed functional connectivity in patients with IESS in terms of spectral power and its effect on treatment responses⁹, to the best of our knowledge, no study has yet investigated topological alterations in patients with IESS using EEG. Therefore, the present study aimed to evaluate the differences in EEG microstates between patients with IESS and healthy controls (HC). We further hypothesized that EEG microstates would vary depending on the etiological characteristics of patients with IESS. Thus, we explored the potential of microstate features as biomarkers by employing machine learning classifiers to distinguish between patients with IESS and HC, and to differentiate between subtypes of IESS based on specific etiology.

Materials and methods
Patient enrollment

This retrospective study enrolled 49 HCs and 42 patients with IESS who all underwent investigation of clinical and electrophysiological characteristics. The study cohort was retrieved from Asan Medical Center, and included patients aged 3–12 months who visited the pediatric neurology clinic. IESS cases were consistent with the 2022 International League Against Epilepsy (ILAE) classification and exhibited hypsarrhythmia on the EEG. The HC group included infants who underwent EEG investigations after visiting the neurology clinic for paroxysmal non-epileptic motor events and achieved normal developmental milestones. Data including age, sex, and etiology were sourced from patients’ electronic medical records (Table 1). This study was reviewed and approved by the Institutional Review Board of the University of Ulsan College of Medicine, Seoul, Korea (IRB No. 2023–0644), and the need for informed consent was waived for all study subjects. All methods were performed in accordance with the relevant guidelines and regulations, as outlined in the approved study protocol.

Patients with IESS were categorized into two groups based on etiological differences: those with structural/metabolic etiologies (Group S) and those with genetic or unknown etiologies (Group NS).

Data acquisition and processing

A 19-channel scalp EEG was recorded using an international 10–20 electrode placement system with a modified combinatorial nomenclature. The subjects were maintained in a sedated sleep state for at least 30 min, induced with an oral dose of 50 mg/kg chloral hydrate. EEG data were collected during the non-REM sleep stage, which was determined by characteristic features, including oculographic findings. A clean five-minute segment, devoid of muscle- or eye-related artifacts, was manually selected for analysis by experienced pediatric neurologists (HNJ, M-JK, and M-SY). Raw EEG data, sampled at a rate of 200 Hz, were re-referenced to a common average reference, and underwent preprocessing involving a 60 Hz notch filter, a 2–20 Hz band-pass filter, and independent component analysis (ICA). Each subject’s EEG data were subsequently divided into fixed-length epochs comprising two-second windows without overlap.

EEG microstate analysis

Five microstate maps were derived from each subject’s global field power (GFP) using modified k-means clustering, a method that disregards polarity during the clustering process¹⁰. Given the inherent instability of K-means clustering, we performed 100 clustering runs with random seeds ranging from 1 to 100 and selected the clustering results that exhibited the highest GEV. The number of microstates was determined using a meta-criterion¹¹ incorporating silhouette (Sil), Calinski-Harabasz (CH), Dunn, and Davies-Bouldin (DB) scores within the range of 4–10^{12–15}. These scores are widely used in the evaluation of clustering performance, and have been employed in previous studies to select the optimal number of clusters^{16,17}. Based on this meta-criterion, five optimal microstates were identified (Supplementary Fig. S1).

In the present study, similar to the methods utilized in quantitative EEG (qEEG) analysis^{18–20}, we employed an approach to identify deviations in the microstate features of patients with IESS from the normative range derived from HCs. To extract microstate maps for HC, we concatenated the microstate maps from each HC subject, and subsequently applied modified k-means clustering. We fitted five microstate maps to the EEG data of each subject to obtain microstate segments, labeling each segment by estimating the spatial correlations with the HC microstate maps. Subsequently, we calculated the various microstate features from the segments of each subject’s EEG, including both HC and patients with IESS. The extracted microstate features included (1)

Variable		Patients with IESS (n = 42)	Healthy control (n = 49)	P-value
Age (months)		7.8 ± 2.5	7.2 ± 2.4	0.24
Sex	Male	19 (45.2%)	23 (46.9%)	0.87
	Female	23 (54.8%)	26 (53.1%)	
Etiology	Structural and/or metabolic	24 (57.1%)	N/A	N/A
	Genetic	9 (21.4%)	N/A	N/A
	Unknown	9 (21.4%)	N/A	N/A
Outcomes	Intractable epilepsy	17 (40.5%)	N/A	N/A

Table 1. Demographics of infantile epileptic spasms syndrome (IESS) and healthy control.

global explained variance (GEV), reflecting the proportion of total EEG signal variance accounted for by each microstate; (2) occurrence, which measures the frequency of each microstate within a specified time period; (3) time coverage, representing the percentage of total presence time for each microstate; and (4) mean durations, indicating the average length of time each microstate was sustained. Additionally, transitional probabilities across the five microstates, which capture the transition patterns between each microstate (e.g., from microstate A to B), were utilized as part of the microstate features. Analyses were conducted using PycroStates¹⁶, a Python library designed to study EEG microstates.

Statistical analysis

Demographic data

The collected data underwent statistical analysis, with normality assessed using the Shapiro-Wilk test. Mann-Whitney U tests and independent t-tests were applied for non-normally and normally distributed data, respectively. The Chi-square test was applied to analyze qualitative variables, and continuous variables were compared between the case and control groups using independent sample t-tests. Statistical significance was set at $P < 0.05$.

Electrophysiological data

We conducted two types of statistical analyses: one comparing the healthy control (HC) group and the infantile epileptic spasms syndrome (IESS) group, and the other comparing the HC, Group NS, and Group S groups.

First, to statistically compare HC and IESS, we employed multivariate analysis of variance (MANOVA) to determine whether there were significant differences in multivariate data between the two groups. Subsequently, to address the multiple comparison issue in multivariate analysis, we performed post-hoc analysis using ANOVA with Bonferroni correction to identify significant differences in each univariate variable between the two groups.

Second, for the statistical comparison among HC, Group NS, and Group S, we assessed multivariate normality using the Henze-Zirkler test, as the sample sizes of Group NS and Group S were relatively small ($n < 30$). The test results indicated that the normality assumption was not satisfied ($P < 0.05$). Therefore, instead of MANOVA, we applied a nonparametric approach, the multivariate Kruskal-Wallis test, to examine whether there were significant differences among the three groups. Similarly, to mitigate the multiple comparison issue in multivariate analysis, we conducted a post-hoc analysis using the Kruskal-Wallis test with Bonferroni correction to identify significant differences in each univariate variable among the three groups. Additionally, to further address the multiple comparison problem when analyzing multiple groups, we applied the Mann-Whitney U-test with Bonferroni correction to determine which specific groups exhibited differences in each univariate variable.

Machine learning analysis

To assess the potential of microstate biomarkers as discriminative features for IESS and its subtypes, we conducted a receiver operating characteristic (ROC) analysis using a machine learning approach. In this analysis, we applied logistic regression with an ElasticNet regularization to prevent overfitting. We standardized the input features and set L1 regularization ratio to 0.2. To validate the classification potential of significant microstate features, we utilized only the features that exhibited statistically significant differences in the statistical analysis as input variables. Subsequently, we analyzed which microstate features contributed the most to classification by investigating the absolute values of the classifier's coefficients. Given the limited amount of data in this study, we implemented leave-one-out cross-validation (LOOCV) and used the area under the curve (AUC) score as the evaluation metric. The AUC score was computed by aggregating the LOOCV results, and the 95% confidence interval (CI) was estimated using bootstrap resampling²¹. For bootstrap resampling, we perform resampling 2000 times.

Results

Demographics and clinical variables

This study enrolled 42 patients with IESS and 49 HCs. The patient demographic data are presented in Table 1. There were no statistically significant differences in age or sex between the groups. Among patients with IESS, the most common etiology was structural/metabolic ($n = 24$, 57.1%), and 17 (40.5%) patients developed intractable epilepsy at the last follow-up.

Altered EEG microstates in healthy controls and patients with IESS

The topological microstate maps independently extracted from HCs and patients with IESS, displayed distinct patterns, particularly in microstate E (Fig. 1). To further investigate the differences between HC and patients with IESS, microstate features were calculated based on microstates A–E, derived from HCs. The MANOVA results indicated that the multivariate microstate features significantly differed between the HC and IESS groups. Specifically, the test statistics for Wilks' lambda, Pillai's trace, Hotelling-Lawley trace, and Roy's greatest root all showed significant differences between the two groups ($P < 0.0001$ for all tests). The GEV for microstates A and B was significantly higher in patients with IESS, whereas it was lower for microstates D and E compared to HC (Fig. 2a, $P < 0.0001$). Significant differences in mean duration were primarily observed in microstates A, B, and D. Specifically, microstates A and B exhibited longer durations in patients with IESS, whereas microstate D had a relatively shorter duration than in HCs (Fig. 2b, $P < 0.0001$). Additionally, microstates A and B occupied a greater percentage of the total time in patients with IESS compared to HCs (Fig. 2c, $P < 0.0001$), whereas microstates D and E demonstrated reduced time coverage. Furthermore, the occurrences of microstates A and B were elevated, whereas those of microstates D and E were reduced in patients with IESS (Fig. 2d, $P < 0.0001$). The p-values of post-hoc ANOVA are shown in Supplementary Table S1.

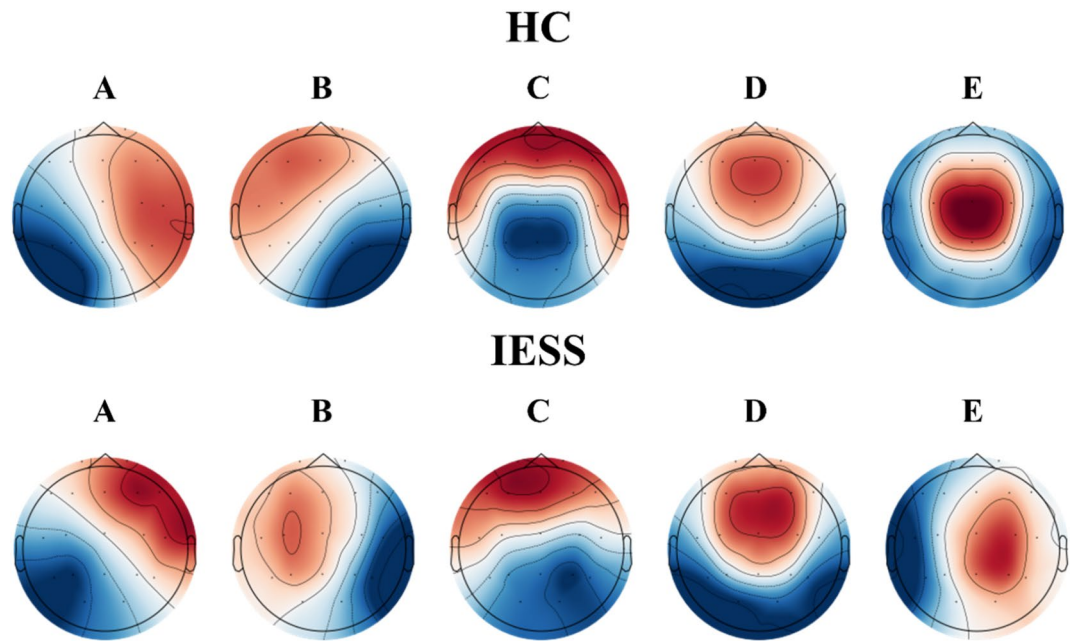


Fig. 1. Topological microstate maps of HC and patients with IESS. The five microstates were derived from k-means clustering across subjects in HC and patients with IESS.

Alterations in EEG microstate based on etiology and seizure outcomes

To investigate the functional differences in microstates based on specific types of IESS, we categorized patients with IESS according to their etiology (Group S: structural and/or metabolic vs. Group NS: genetic and unknown) and outcomes (intractable epilepsy vs. controlled epilepsy), as shown in Table 1. Group S, comprising patients with structural/metabolic etiologies, accounted for 24 of the total IESS cases, whereas Group NS, comprising those with genetic and unknown etiologies, included 18 cases. The multivariate Kruskal-Wallis test showed that the multivariate microstate features exhibited significant differences among the IESS, Group NS, and Group S groups ($P < 0.0001$) (Supplementary Table S2). However, post-hoc analysis using the Kruskal-Wallis test with Bonferroni correction revealed that all variables of microstate C and the mean duration of microstate E did not show significant differences among the groups (Supplementary Table S3). Patients in Group S exhibited the highest GEV, mean duration, occurrence, and time coverage in microstate A compared to the NS and HC groups, indicating a greater deviation from normalcy. In contrast, microstate D displayed the lowest time coverage and occurrence in Group S, followed by the NS and HC groups (Fig. 3). Specifically, in microstate A, all four microstate features in Group S differed significantly from those in both HC and NS groups. In microstate D, significant differences were observed between the S and NS groups in terms of time coverage and occurrence. The p-values of post-hoc Mann-Whitney U-test are shown in Supplementary Table S4.

Of the patients with IESS, 17 were confirmed to have intractable epilepsy at the final follow-up; however, no significant differences were found between the controlled and intractable epilepsy groups regarding GEV, mean duration, time coverage, and occurrence (Supplementary Fig. S2, Table S5).

Transition probability of microstates

Transitions between microstates reflect the sequential synchronized activity of various neural networks. Figure 4 (a) presents the differences in transition probabilities between the HC and IESS. The MANOVA results showed significant differences in the multivariate transition probabilities between the HC and IESS groups. All test statistics, including Wilks' lambda, Pillai's trace, Hotelling-Lawley trace, and Roy's greatest root, indicated statistically significant differences between the two groups ($P < 0.0001$ for all tests). Transition probabilities from microstates B, C, D, and E toward A were significantly higher in IESS ($P < 0.0001$), whereas the probabilities of transitioning from microstates A, B, C, and E toward D and microstates A, B, C, and D toward E were lower in patients with IESS ($P < 0.05$) (Supplementary Table S1).

In the analysis of patients with different etiologies between Groups S and NS (Fig. 4b), the multivariate Kruskal-Wallis test indicated significant differences in the multivariate transition probabilities among the IESS, Group NS, and Group S groups ($P < 0.0001$) (Supplementary Table S2). However, post-hoc analysis using the Kruskal-Wallis test with Bonferroni correction revealed no significant differences in the transition probabilities from microstates A, B, and E toward C, as well as from microstate D toward B, across the groups. (Supplementary Table S3). Transition probabilities indicated the likelihood of switching from microstates B, C, and D toward A were found to be increased in Group S, while those from C to D were decreased ($P < 0.05$) (Supplementary Table S4).

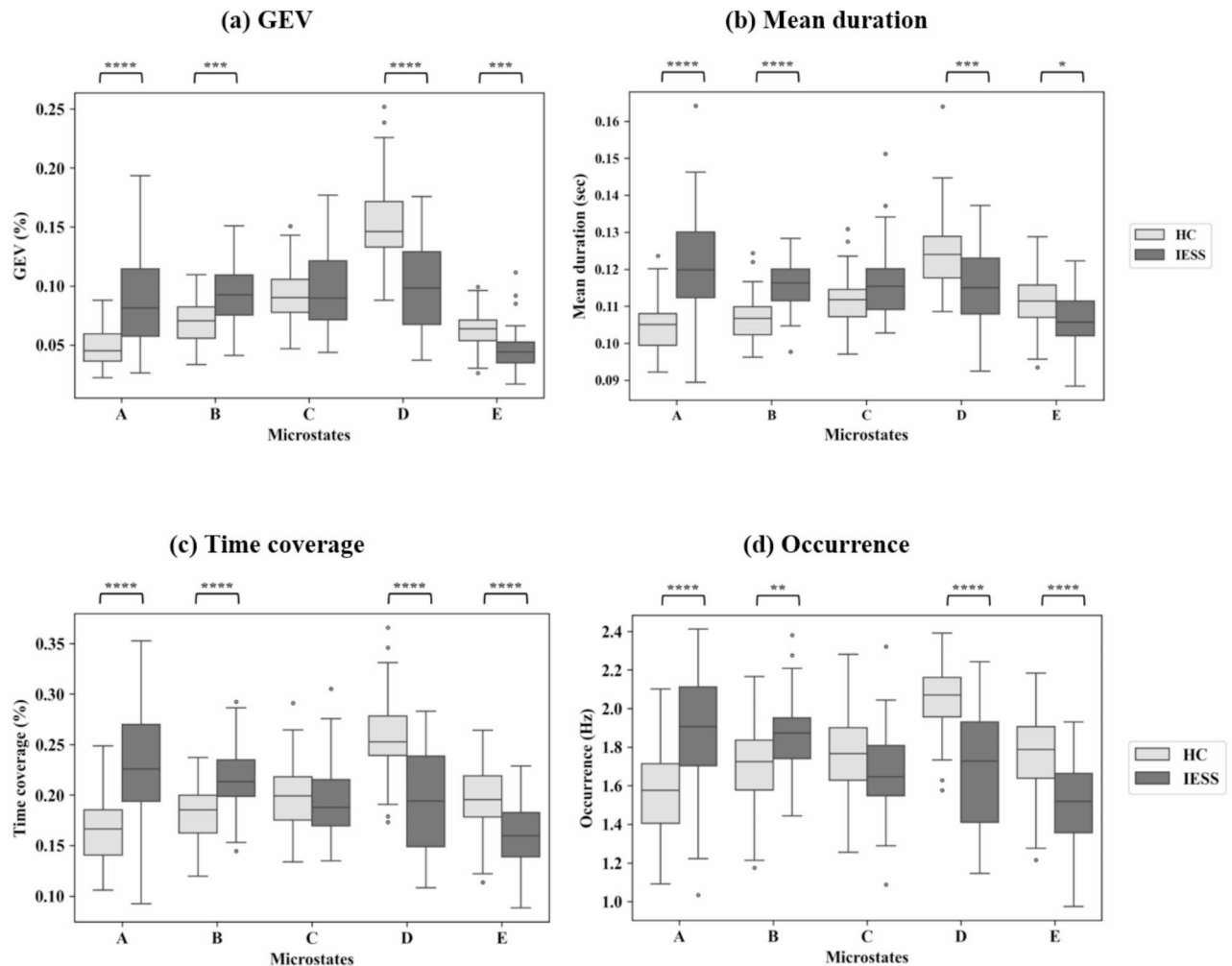


Fig. 2. Comparisons of microstate features between IESS and patients with HC. **(a)** Global explained variance (GEV), **(b)** Mean duration, **(c)** Time coverage, and **(d)** Occurrence. Asterisks indicate statistical significance (* $P < 0.05$, ** $P < 0.01$, *** $P < 0.001$, **** $P < 0.0001$).

IESS classification using machine learning approach

We applied machine learning methods to assess the predictive capability of features extracted from the microstate analysis and to demonstrate their significance as biomarkers. Specifically, we applied logistic regression with ElasticNet regularization to develop two models: the IESS classifier, which distinguishes between HC and patients with IESS, and the IESS etiology classifier, which differentiates between Group S (structural/metabolic etiology) and Group NS (genetic and unknown etiology). In addition, we investigated which microstate features contributed the most to classification through feature importance. Feature importance was calculated based on the absolute values of classifier's coefficients. The confusion matrix for each classifier is presented in Supplementary Fig. S3.

Classification between HC and IESS

The IESS classifier demonstrated high predictive performance, with an AUC of 0.91 (0.83–0.96) (Fig. 5a). The top five most important features included the transition probability from A to D, the mean duration of microstate A, the occurrence of microstates E and B, and the global explained variance (GEV) of microstate D (Fig. 5b). These features exhibited notably high importance, implying a significant role in classification. Conversely, the five least important features comprised the time coverage of microstates A and D, the transition probability from E to A and from B to E, and the mean duration of microstate E. These features exhibited very low importance, indicating a negligible impact on classification. Overall, the features associated with microstates A and D were highly important in distinguishing HC from IESS (sensitivity = 0.76, specificity = 0.90).

Classification based on patient etiologies

The IESS etiology classifier demonstrated notable predictive performance with an AUC of 0.71 (0.54–0.86) (Fig. 6a). The six most influential features included the transition probabilities from C to D, B to A, D to A, and C to A, along with the time coverage of microstate D (Fig. 6b). These features demonstrated particularly

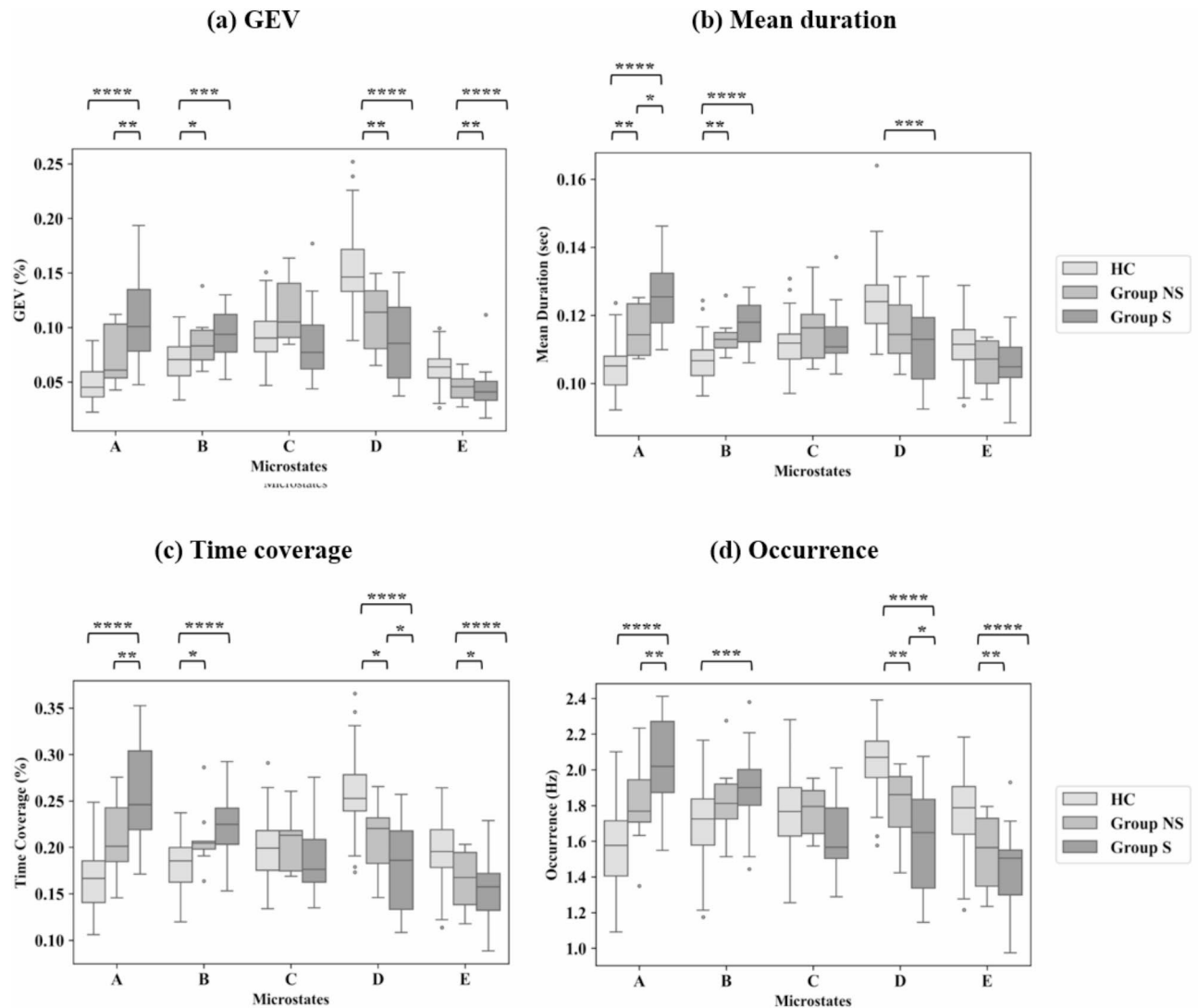


Fig. 3. Altered EEG microstates in HC, Group S (structural and metabolic patient group), and Group NS (genetic and unknown patient group). **(a)** Global explained variance (GEV), **(b)** Mean duration, **(c)** time coverage, and **(d)** occurrence. Asterisks indicate statistical significance (* $P < 0.05$, ** $P < 0.01$, *** $P < 0.001$, **** $P < 0.0001$).

high importance, highlighting their substantial role in classification. Notably, the transition probability features involving microstates A and D were identified as especially informative. Conversely, the three least significant features were the mean duration of microstate A, the occurrence of microstate A, and its time coverage. These features exhibited minimal importance, suggesting a negligible effect on classification. Overall, transition probability features related to microstate A played a pivotal role in differentiating etiologies (sensitivity = 0.79, specificity = 0.61).

Discussion

This study explored the topological changes in patients with IESS through EEG microstate analysis, making the first comparison between patients with IESS and HC. Significant alterations were observed in microstates A, B, D, and E, indicating disrupted brain networks in IESS, particularly in patients with structural/metabolic etiologies. Overall, our analyses showed that the features of microstates A and B exhibited significant increases in GEV, duration, occurrence, and coverage in patients with IESS compared to HCs, whereas the opposite was observed for microstates D and E (Fig. 2). In contrast, microstate C did not show significant differences between the two groups. In subgroup analyses, microstate A was found to be significantly elevated in patients with structural/metabolic etiologies (Group S) compared to those with genetic/unknown etiologies (Group NS), exhibiting increases in all four features. Conversely, microstate D demonstrated decreased occurrence and time coverage in Group S compared to Group NS (Fig. 3). Our findings indicate that microstates A and B are more pronounced in patients with IESS, while microstates D and E exhibit reductions in IESS compared to HCs. These topological

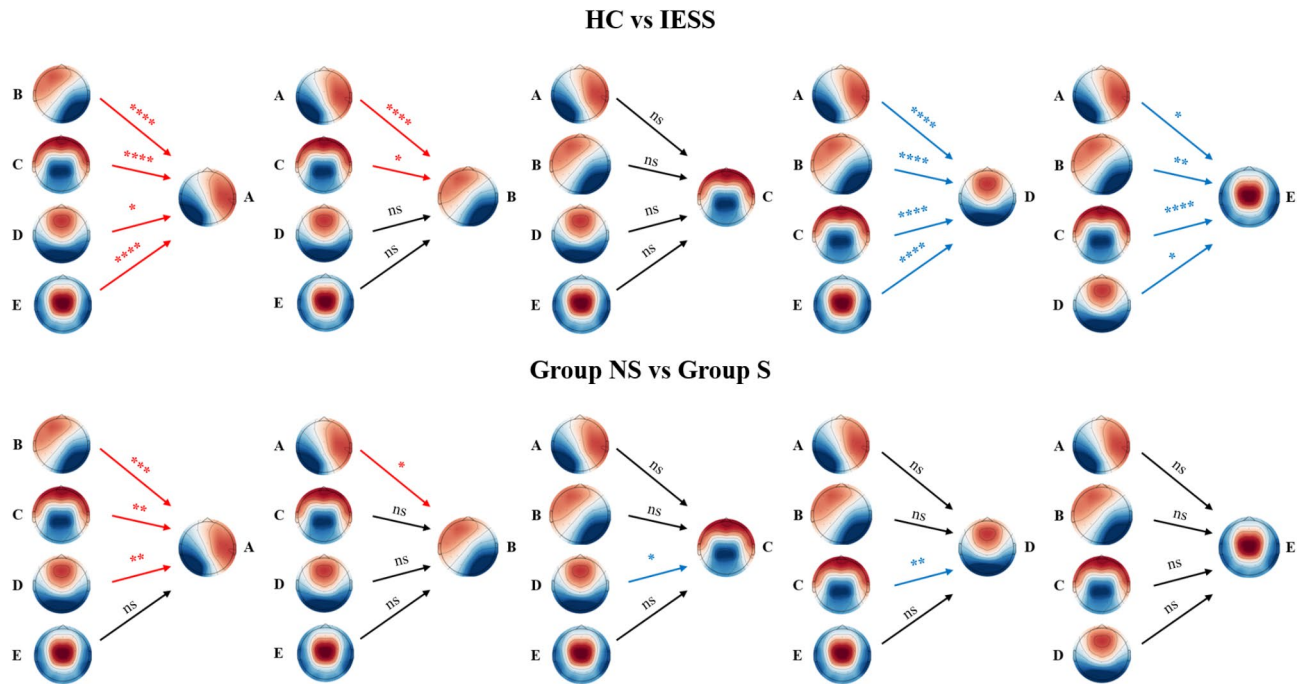


Fig. 4. Transition probabilities for (a) the HC and IESS groups and (b) Group S and Group NS. Asterisks are shown on each transitional arrow, with asterisks indicating statistical significance (* $P < 0.05$, ** $P < 0.01$, *** $P < 0.001$, **** $P < 0.0001$). The 'ns' indicates not significant. Red P-values indicate larger values in the second group (i.e. IESS or Group S), while blue P-values indicate smaller values in the second group.

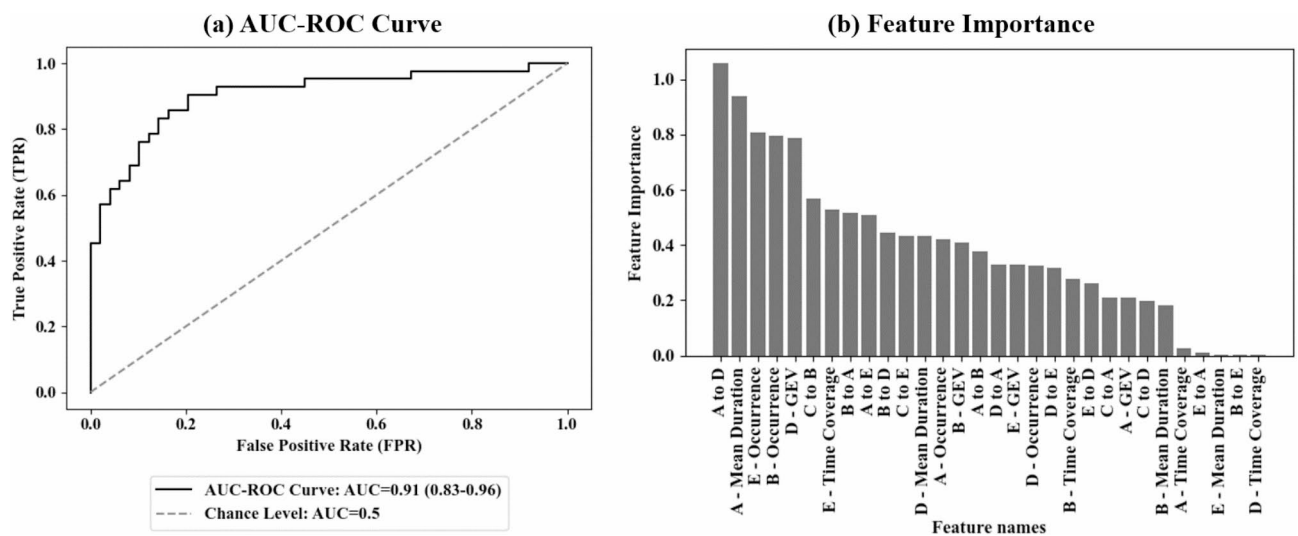


Fig. 5. Machine learning analysis for discrimination between IESS and HC. (a) AUC-ROC curve for the IESS classifier (AUC=0.91 (0.83–0.96)). (b) Feature importance for IESS classification.

alterations in microstate dynamics reflect disrupted brain networks in patients with IESS, particularly those with a structural/metabolic etiology. In this study, we further analyzed transition probabilities to examine how frequently the brain switches between different functional states. Our results revealed significant differences in transition probabilities between HCs and patients with IESS, particularly with higher transition probabilities from all other microstates (B, C, D, and E) to microstate A in IESS. This pattern suggests a disruption in brain function and abnormal network connectivity, potentially indicating an over-reliance on microstate A in IESS. Furthermore, Group S exhibited higher transition probabilities to microstate A than Group NS, indicating etiology-related differences. Given that we also observed significant differences in the GEV, duration, occurrence, and time coverage of microstate A, its role in brain network dynamics should be further investigated.

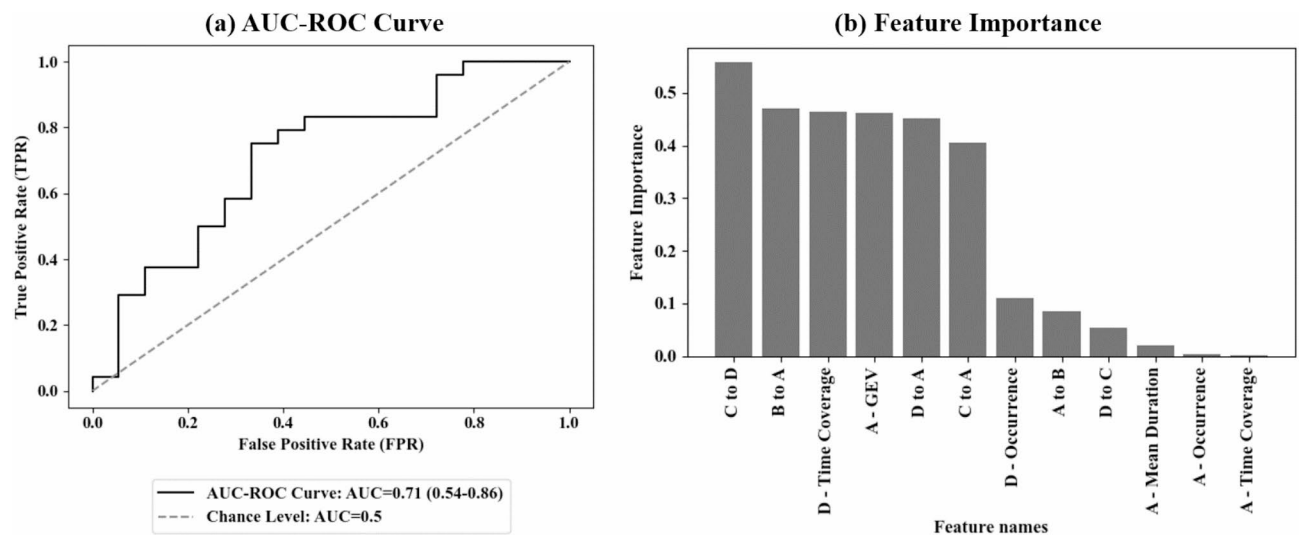


Fig. 6. Machine learning analysis for discrimination between Group S and Group NS. **(a)** AUC-ROC Curve for the IESS etiology classifier (AUC = 0.71 (0.54–0.86)). **(b)** Feature importance for etiology classification.

EEG microstate analysis has been previously proven useful in multiple neurological and psychiatric disorders, including epilepsy. Each microstate is thought to correspond to the functional anatomical relationships within different brain regions. Specifically, microstates A, B, C, and D are associated with the auditory or somatosensory–motor network, the visual network, the salience network, and the attention networks, respectively^{22,23}. Jiang et al. reported that patients with idiopathic (or genetic) generalized epilepsy (IGE) with ongoing seizures displayed an increased frequency and coverage of microstate A compared to HCs and seizure-free IGE patients²⁴. The authors suggested that this finding can be associated with increased synchrony in the sensorimotor network in IGE. In our study, similar patterns were observed in patients with IESS with even greater alteration in microstate A in patients in Group S, indicating that patient with structural etiology may result in a relative enhancement of sensorimotor network dynamics when compared to other networks. In another study investigating EEG microstate abnormalities based on temporal lobe epilepsy (TLE) subtypes, patients with bilateral TLE exhibited a significant increase in microstate A and a decrease in microstate D compared to both patients with unilateral TLE and HCs²⁵. In bilateral TLE, microstate A has been associated with abnormal activation of bilateral temporal regions and progressive network reorganization over time. Similarly, structural alteration in group S in our study may induce widespread functional changes beyond the primary lesions, potentially leading to microstate A becoming a more dominant attractor in the system. Moreover, the dominance of microstate A in Group S may be reflective of network alterations underlying epileptic encephalopathy in IESS. In light of previous studies reporting microstate alteration with normal brain MRI in IGE, TLE, and AE, this increased prominence of microstate A could serve as an early indicator of functional alterations in patients with epilepsy. The authors also suggested the potential association between reduced microstate D and impaired cognitive processes in patients with bilateral TLE²⁵. Similarly, in our study, patients with IESS exhibited reduced microstate D dynamics, particularly in Group S. Moreover, we observed that profound developmental delay was associated with a reduced transition probability from microstate A to microstate D, a pattern consistent with the trend observed in the comparison between HC and IESS (Supplementary Fig. S4, Table S6). While this does not directly confirm a decrease in microstate D itself, it suggests a potential disruption in the neural dynamics involving microstate D. However, as profound delay was not significantly associated with etiologies in our dataset, further research incorporating neurophysiologic studies such as, intellectual quotient (IQ) assessment is needed to determine how microstate D alterations may differentially manifest across etiologies.

In the present study, we conducted a machine learning analysis based on significance results obtained by statistical tests to explore the diagnostic potential of microstate features and transitional probabilities as biomarkers. The IESS classifier exhibited high performance, achieving an AUC of 0.90, highlighting the discriminative power of microstate dynamics (Fig. 5). As the first microstate study to examine IESS, our model demonstrated high performance compared with a previous microstate study on patients with TLE, which reported a model accuracy of 76.1%²⁶. Another study that utilized transitional probabilities as features for machine learning achieved 84.72% accuracy in differentiating between patients with TLE and HCs²⁷. Furthermore, our approach achieved moderate yet notable performance in classifying patient etiologies, with an AUC of 0.71 (Fig. 6). The results were comparable to those of another study that differentiated focal epilepsy from PNES types with an AUC of 0.78²⁸. In the feature importance analysis, features related to microstate A and D were particularly influential in both classifiers (Figs. 5b and 6b). Specifically, transitional probabilities involving these two microstates played a key role as distinguishing biomarkers. This suggests that microstate A and D may be linked to structural abnormalities in the developing brain, consistent with statistical results presented above. These findings highlight the potential of EEG microstate analysis as a cost-effective, non-invasive tool for identifying IESS in clinical settings and investigating dynamic neural mechanisms underlying

the disorder. Given its high temporal resolution, EEG microstate analysis may also enable early detection of neurophysiological abnormalities before structural changes become apparent on brain imaging such as MRI.

While our findings highlight specific microstate alterations in IESS, their clinical implications remain uncertain. Given that each microstate reflect specific functional networks within the brain, their relevance may extend beyond epilepsy classification to broader functional outcomes, such as neurodevelopment and treatment response. Typical spasms with hypsarrhythmia on EEG have been identified as diagnostic indicators of IESS. Patients with hypsarrhythmia are more likely to experience adverse effects on brain development; if left untreated, it can result in intellectual disability or developmental delays. However, changes in microstates in IESS patients do not correlate with final epilepsy outcomes (Supplementary Fig S2, Table S5). This may suggest that microstates could be associated with other outcomes, such as language development, intellectual disability, spasm control with specific anti-seizure medications, or current brain function status, including structural abnormalities and developmental progress^{29,30}. Several studies have reported associations between microstate alterations and treatment response in epilepsy. For example, altered microstates have been associated with specific anti-seizure medications (ASMs), such as perampanel, in drug-resistant epilepsy³¹. In the seizure-free group, a decrease in the duration and coverage of microstate A, as well as in the frequency and coverage of microstate B, was observed, along with reductions in the duration, frequency, and the coverage of microstate C. In a study examining the effects of levetiracetam in patients newly diagnosed with TLE, pre- and post-treatment EEG microstate analysis demonstrated a reduction in the mean duration and occurrence of microstates B and D following treatment, with a directional predominance of transitions from microstates A to C and from microstates B to D³². However, in our study, microstates did not distinguish between treatment responsiveness or seizure intractability. This discrepancy may stem from the heterogeneity of treatment regimens, the complexity of seizure pathophysiology, or the limited sample size. Nonetheless, with a larger dataset and more controlled clinical conditions, further research may uncover microstate patterns predictive of treatment outcomes in IESS.

Methodologically, our study offers a unique contribution compared to previous research, as this is the first study to describe topological alterations using EEG-based microstate analysis in patients with IESS, including an age-matched HCs. To select the relevant microstates, we used the GEV and rank sum of the five clustering evaluation metrics to determine the optimal set of microstates. Therefore, this combination ensured that the selected microstates effectively explained the EEG data and formed distinct, well-defined patterns. We applied a bandpass filter between 2 and 20 Hz, a frequency range that has been shown to capture spontaneous, resting-state activity relevant to global network organization.

Nevertheless, our study had several limitations. Firstly, the cohort sample size was relatively small, and abnormalities in brain MRI, which could reflect the morphological status of the study group, were not included for the analysis. Due to the small sample size, we were unable to observe significant differences across the different etiology groups, such as genetic, metabolic, structural, and unknown. However, as highlighted in previous pediatric brain MRI analyses, metabolic diseases affecting the pediatric brain are complex, with diverse underlying mechanisms that lead to structural damage³³ and can be categorized as structural etiology³⁴. Additionally, the patients categorized under metabolic etiology in this study had structural brain lesions. Thus, we grouped metabolic and structural etiologies together while distinguishing them from non-structural etiologies. When examining the differences between the unknown and genetic etiology groups, no statistically significant differences were found, although a prominent microstate alteration was observed in the structural etiology group.

Additionally, all patients in the study were administered an oral dose of 50 mg/kg chloral hydrate. The confounding effects of neuroactive drugs on brain topological alterations may have been underestimated. Lastly, differences in microstates could not be directly associated with specific brain connectivity. Therefore, careful clinical interpretation and further functional investigation are required.

Despite these limitations, we observed significant differences and moderate machine-learning performance in distinguishing between HC and IESS, particularly among patients with structural/metabolic etiologies. These findings indicate that applying microstate analysis to patients with IESS could provide a deeper understanding of brain network dysfunction, enhance diagnostic accuracy, monitor treatment effectiveness, and identify predictive biomarkers for cognitive outcomes.

Conclusion

In conclusion, the present study provides valuable insights into the EEG microstate dynamics of patients with IESS. Notably, microstate A and transition probabilities toward microstate A emerged as defining features of IESS, particularly among patients with structural/metabolic etiologies. These findings indicate disrupted brain connectivity in the sensorimotor and auditory networks, thereby offering further insights into the need for novel analytical approaches.

Data availability

The data of this study are available upon request from the corresponding author, subject to approval under the guidelines of the Institutional Review Board (IRB).

Received: 11 December 2024; Accepted: 6 March 2025

Published online: 19 March 2025

References

1. Zuberi, S. M. et al. ILAE classification and definition of epilepsy syndromes with onset in neonates and infants: position statement by the ILAE task force on nosology and definitions. *Epilepsia* **63**, 1349–1397. <https://doi.org/10.1111/epi.17205> (2022).

2. Bernhardt, B. C., Hong, S., Bernasconi, A. & Bernasconi, N. Imaging structural and functional brain networks in Temporal lobe epilepsy. *Front. Hum. Neurosci.* **7**, 624. <https://doi.org/10.3389/fnhum.2013.00624> (2013).
3. Wang, Y., Li, Y., Yang, L. & Huang, W. Altered topological organization of resting-state functional networks in children with infantile spasms. *Front. Neurosci.* **16** <https://doi.org/10.3389/fnins.2022.882227> (2022).
4. Moeller, F., Stephani, U. & Siniatchkin, M. Simultaneous EEG and fMRI recordings (EEG-fMRI) in children with epilepsy. *Epilepsia* **54**, 971–982. <https://doi.org/10.1111/epi.12215> (2013).
5. Shrey, D. W. et al. Strength and stability of EEG functional connectivity predict treatment response in infants with epileptic spasms. *Clin. Neurophysiol.* **129**, 2137–2148. <https://doi.org/10.1016/j.clinph.2018.07.006> (2018).
6. Dickinson, A. et al. Multivariate neural connectivity patterns in early infancy predict later autism symptoms. *Biol. Psychiatry Cogn. Neurosci. Neuroimaging* **6**, 59–69. <https://doi.org/10.1016/j.bpsc.2020.05.002> (2021).
7. Michel, C. & Koenig, T. EEG microstates as a tool for studying the Temporal dynamics of whole-brain neuronal networks: a review. *Neuroimage* **180**, 577–593. <https://doi.org/10.1016/j.neuroimage.2017.06.031> (2017).
8. Khanna, A., Pascual-Leone, A., Michel, C. M. & Farzan, F. Microstates in resting-state EEG: current status and future directions. *Neurosci. Biobehav. Rev.* **49**, 105–113. <https://doi.org/10.1016/j.neubiorev.2014.12.010> (2015).
9. Kim, J., Kim, M. J., Kim, H. J., Yum, M. S. & Ko, T. S. Electrophysiological network predicts clinical response to Vigabatrin in epileptic spasms. *Front. Neurol.* **14**, 1145077. <https://doi.org/10.3389/fneur.2023.1145077> (2023).
10. Pascual-Marqui, R. D., Michel, C. M. & Lehmann, D. Segmentation of brain electrical activity into microstates: model Estimation and validation. *IEEE Trans. Biomed. Eng.* **42**, 658–665. <https://doi.org/10.1109/10.391164> (1995).
11. Custo, A. et al. Electroencephalographic resting-state networks: source localization of microstates. *Brain Connect.* **7**, 671–682. <https://doi.org/10.1089/brain.2017.0510> (2017).
12. Rousseeuw, P. J. Silhouettes: a graphical aid to the interpretation and validation of cluster analysis. *J. Comput. Appl. Math.* **20**, 53–65. [https://doi.org/10.1016/0377-0427\(87\)90125-7](https://doi.org/10.1016/0377-0427(87)90125-7) (1987).
13. Caliński, T. & Harabasz, J. A dendrite method for cluster analysis. *Commun. Stat. Theory Methods* **3**, 1–27. <https://doi.org/10.1080/03610927408827101> (1974).
14. Dunn, J. C. Well-separated clusters and optimal fuzzy partitions. *J. Cybern.* **4**, 95–104. <https://doi.org/10.1080/01969727408546059> (1974).
15. Davies, D. L. & Bouldin, D. W. A cluster separation measure. *IEEE Trans. Pattern Anal. Mach. Intell.* **2**, 224–227. <https://doi.org/10.1109/TPAMI.1979.4766909> (1979).
16. Férat, V., Scheltienne, M., Brunet, D., Ros, T. & Michel, C. Pycrostates: a Python library to study EEG microstates. *J. Open. Source Softw.* **7**, 4564. <https://doi.org/10.21105/joss.04564> (2022).
17. Huang, Z., Zhang, J., Wu, J., Mashour, G. A. & Hudetz, A. G. Temporal circuit of macroscale dynamic brain activity supports human consciousness. *Sci. Adv.* **6**, eaaz0087. <https://doi.org/10.1126/sciadv.aaz0087> (2020).
18. Lin, L. C., Ouyang, C. S., Chiang, C. T., Wu, H. C. & Yang, R. C. Early evaluation of the therapeutic effectiveness in children with epilepsy by quantitative EEG: a model of mozart K. 448 listening—a preliminary study. *Epilepsy Res.* **108**, 1417–1426. <https://doi.org/10.1016/j.epilepsyres.2014.08.003> (2014).
19. Ouyang, C. S. et al. Quantitative EEG findings and response to treatment with antiepileptic medications in children with epilepsy. *Brain Dev.* **40**, 26–35. <https://doi.org/10.1016/j.braindev.2017.09.007> (2018).
20. Ricci, L. et al. Measuring the effects of first antiepileptic medication in Temporal lobe epilepsy: predictive value of quantitative EEG analysis. *Clin. Neurophysiol.* **132**, 25–35. <https://doi.org/10.1016/j.clinph.2020.10.018> (2021).
21. Carpenter, J. & Bithell, J. Bootstrap confidence intervals: when, which, what? A practical guide for medical statisticians. *Statist Med.* **19**, 1141–1164 (2000).
22. Britz, J., Van De Ville, D. & Michel, C. M. BOLD correlates of EEG topography reveal rapid resting-state network dynamics. *Neuroimage* **52**, 1162–1170. <https://doi.org/10.1016/j.neuroimage.2010.02.052> (2010).
23. Yuan, H., Zotev, V., Phillips, R., Drevets, W. C. & Bodurka, J. Spatiotemporal dynamics of the brain at rest—exploring EEG microstates as electrophysiological signatures of BOLD resting state networks. *Neuroimage* **60**, 2062–2072. <https://doi.org/10.1016/j.neuroimage.2012.02.031> (2012).
24. Jiang, Y., Zhu, M., Hu, Y. & Wang, K. Altered resting-state electroencephalography microstates in idiopathic generalized epilepsy: a prospective case-control study. *Front. Neurol.* **12**, 619048. <https://doi.org/10.3389/fneur.2021.619048> (2021).
25. Baldini, S. et al. Electroencephalographic microstates as a potential neurophysiological marker differentiating bilateral from unilateral Temporal lobe epilepsy. *Epilepsia* **65**, 664–674. <https://doi.org/10.1111/epi.17679> (2024).
26. KR, V. et al. Machine learning detects EEG microstate alterations in patients living with Temporal lobe epilepsy. *Seizure* **61**, 8–13. <https://doi.org/10.1016/j.seizure.2018.07.005> (2018).
27. Feng, R. et al. Spatiotemporal microstate dynamics of spike-free scalp EEG offer a potential biomarker for refractory Temporal lobe epilepsy. *IEEE Trans. Med. Imaging*. <https://doi.org/10.1109/TMI.2024.0000000> (2024).
28. Kucikienė, D. et al. EEG microstates show different features in focal epilepsy and psychogenic nonepileptic seizures. *Epilepsia* **65**, 974–983. <https://doi.org/10.1111/epi.17688> (2024).
29. Riikonen, R. S. Favourable prognostic factors with infantile spasms. *Eur. J. Paediatr. Neurol.* **14**, 13–18. <https://doi.org/10.1016/j.ejpn.2008.11.011> (2010).
30. Demarest, S. T. et al. The impact of hypsarrhythmia on infantile spasms treatment response: observational cohort study from the National infantile spasms consortium. *Epilepsia* **58**, 2098–2103. <https://doi.org/10.1111/epi.13912> (2017).
31. Zhu, C. et al. Intrinsic brain activity differences in perampanel-responsive and non-responsive drug-resistant epilepsy patients: an EEG microstate analysis. *Ther. Adv. Neurol. Disord.* **17**, 17562864241227293. <https://doi.org/10.1177/17562864241227293> (2024).
32. Ricci, L. et al. Levetiracetam modulates EEG microstates in Temporal lobe epilepsy. *Brain Topogr.* **35**, 680–691. <https://doi.org/10.1007/s10548-022-00892-5> (2022).
33. Patay, Z. et al. Neurometabolic diseases of childhood. *Pediatr. Radiol.* **45** (Suppl 3), 473–484. <https://doi.org/10.1007/s00247-015-3279-y> (2015).
34. Cascino, G. D., Sirven, J. I., Tatum, W. O. & Epilepsy Second Edition. wiley, 511 p. (2021). <https://doi.org/10.1002/9781119431893>.

Acknowledgements

This research was supported by a grant of Patient-Centered Clinical Research Coordinating Center (PACEN) funded by the Ministry of Health & Welfare, Republic of Korea (grant number: RS-2020-KH096139). This research was also supported by the National Research Foundation of Korea Grant funded by the Ministry of Science and ICT (grant number: NRF-2021R1G1A1094236).

Author contributions

D-HJ and M-SY conceptualized and supervised this study and acquired funding for this study. S-HA analyzed and interpreted the data, provided statistical analysis, and drafted the method. HNJ acquired the data, analyzed and interpreted the data, provided statistical analysis, had full access to all the data in the study, was responsible for the integrity of the data and accuracy of the data analysis, and drafted the manuscript. M-JK acquired and

interpreted the data. SK analyzed and interpreted the data and drafted the machine learning results. All the authors have read and approved the final version of this manuscript.

Declarations

Competing interests

The authors declare no competing interests.

Ethics approval

This study was approved by the Institutional Review Board (IRB No. 2023 – 0644), and the need for informed consent was waived for all study subjects.

Additional information

Supplementary Information The online version contains supplementary material available at <https://doi.org/10.1038/s41598-025-93385-8>.

Correspondence and requests for materials should be addressed to M.-S.Y. or D.-H.J.

Reprints and permissions information is available at www.nature.com/reprints.

Publisher's note Springer Nature remains neutral with regard to jurisdictional claims in published maps and institutional affiliations.

Open Access This article is licensed under a Creative Commons Attribution-NonCommercial-NoDerivatives 4.0 International License, which permits any non-commercial use, sharing, distribution and reproduction in any medium or format, as long as you give appropriate credit to the original author(s) and the source, provide a link to the Creative Commons licence, and indicate if you modified the licensed material. You do not have permission under this licence to share adapted material derived from this article or parts of it. The images or other third party material in this article are included in the article's Creative Commons licence, unless indicated otherwise in a credit line to the material. If material is not included in the article's Creative Commons licence and your intended use is not permitted by statutory regulation or exceeds the permitted use, you will need to obtain permission directly from the copyright holder. To view a copy of this licence, visit <http://creativecommons.org/licenses/by-nc-nd/4.0/>.

© The Author(s) 2025